Research Article

Title: CTLA-4 antibody-drug conjugate reveals autologous destruction of B-lymphocytes associated with regulatory T cell impairment

Authors: Musleh M. Muthana[1,3]*, Xuexiang Du[1,6], Mingyue Liu[1,3], Xu Wang[1,3], Wei Wu[1,7], Chunxia Ai[1,6], Lishan Su[1,2,3,4], Pan Zheng[1,5,7]* and Yang Liu[1,5,7]*

Affiliations:

[1]Division of Immunotherapy, Institute of Human Virology, University of Maryland School of Medicine; Baltimore, MD 21201, USA.

[2]Division of Virology, Pathogenesis and Cancer, Institute of Human Virology, University of Maryland School of Medicine; Baltimore, MD 21201, USA

[3]Department of Pharmacology, University of Maryland School of Medicine; Baltimore, MD 21201, USA

[4]Department of Microbiology & Immunology, University of Maryland School of Medicine; Baltimore, MD 21201, USA

[5]Department of Surgery, University of Maryland School of Medicine; Baltimore, MD 21201, USA.

[6]Key Laboratory of Infection and Immunity of Shandong Province & Department of Immunology, School of Basic Medical Sciences, Shandong University, Jinan, 250012, China

[7]OncoC4, Inc.; Rockville, MD 20805, USA.

[*]Corresponding authors. Email: pzheng@oncoc4.com (PZ); yangl@oncoc4.com (YL); mmuthana@ihv.umaryland.edu (MMM)

Abstract: Germline CTLA-4 deficiency causes severe autoimmune diseases characterized by dysregulation of Foxp3^{+} Tregs, hyper-activation of effector memory T cells, and variable forms autoimmune cytopenia including gradual loss of B cells. Cancer patients with severe immune-related adverse events (irAE) after receiving anti-CTLA-4/PD-1 combination immunotherapy also have markedly reduced peripheral B cells. The immunological basis for B cell loss remains unexplained. Here we probe the decline of B cells in human CTLA-4 knock-in mice by using anti-human CTLA-4 antibody Ipilimumab conjugated to a drug payload emtansine (Anti-CTLA-4 ADC). The anti-CTLA-4 ADC-treated mice have T cell hyper-proliferation and their differentiation into effector cells which results in B cell depletion. B cell depletion is mediated by both CD4 and CD8 T cells and at least partially rescued by anti-TNF-alpha antibody. These data revealed an unexpected antagonism between T and B cells and the importance of regulatory T cells in preserving B cells.

INTRODUCTION

Foxp3 is a master regulator of regulatory T cells (Tregs) and its mutations result in fatal autoimmune disease in mice and human.[1-5] Among many known functions, Foxp3 is a transcriptional factor for expression of CTLA-4, which is constitutively expressed in Tregs.[6,7] *Ctla4* deletion in mice phenocopies that of Foxp3. In humans, CTLA-4 deficiency caused by autosomal heterozygous mutation of the CTLA-4 gene[8,9] or mutations in recycling partner LPS-Responsive beige-like anchor (LRBA) protein[10] are associated with severe autoimmune diseases. Although CTLA-4 can be expressed at lower levels in other cell types and has been suggested as a negative regulator for naïve T cell activation, specific deficiency of CTLA-4 in $Foxp3^+$ Tregs results in development of systemic lymphoproliferation, fatal autoimmune disease, and potent tumor immunity.[11] These data are consistent with the notion that the predominant function of CTLA-4 is Treg-intrinsic.

A largely overlooked area is the cross-regulation between B cells and regulatory T cells. CTLA-4 conditional null mice and those with depletion of Tregs showed increase in germinal center B cells and heightened antibody responses with some reports showing a decrease B cell percentage.[12-15] B cell loss is a common feature in genetic mutations of Foxp3, scurfy mice, Foxp3 knockout mice or Treg depletion.[16-21] Among cancer patients who received immunotherapy, early change of circulating B cells of patients who received combination immunotherapy anti-CTLA-4/PD-1 correlated to irAE.[22] The change in B cells included decline of circulating B cells, and increase in CD21 low B cells and plasmablasts.[22]

The correlation between B cell reduction and immune activation associated with defective Foxp3-CTLA-4 function remains unexplained. Since both CTLA-4 and Foxp3 are largely expressed outside of B cell compartment, and since this pathway is the master regulatory of Treg

function, we hypothesized that B cell loss maybe associated with activation of T cells that are autodestructive of B cells. This hypothesis is noteworthy as no autodestructive T cells for B cells have been described. To test this hypothesis, we generated anti-CTLA-4 ADC and showed that the ADC caused selective depletion of Tregs in mice and a marked reduction of B cells. Remarkably, activation of CD4 and CD8 T cells is the underlying cause of B cell depletion. Our data explains the B cell loss associated with Foxp3 and CTLA-4 dysfunction and suggested an unexpected antagonism between T cells and B cells.

RESULTS

CTLA-4 antibody-drug conjugate depleted regulatory T cells and B cells

Anti-CTLA-4 antibody Ipilimumab (Ipi) or human IgGFc (hIgGFc) control were conjugated to a well-known drug payload DM1, emtansine, to furnish the corresponding ADCs: Ipilimumab-DM1 (Ipi-DM1) and hIgGFc-DM1 with corresponding size shifts in the SDS-gel (Figure 1A). The drug to antibody ratio (DAR) was calculated based on experimentally determined extinction coefficient A280 & A252 for each antibody and reported values for DM1 (Table S1). The DAR from various conjugation is ~3.2 for Ipi-DM1 and ~ 1.7 for hIgGFc-DM1 control (Table S1), as expected based on the sizes of the proteins. The binding for Ipi-DM1 ADC was evaluated by ELISA binding to immobilized His-hCTLA-4 and by flow cytometry using hCTLA-4 expressing CHO cells (CHO-hCTLA-4). Ipi-DM1 binding was found comparable to the parent antibody Ipi (Figures 1B, 1C). Specific killing of CTLA-4-expressing cells by Ipi-DM1 was assessed in human CTLA-4 expressing CHO (CHO-hCTLA-4) and wild type CHO (CHO-WT) cells in vitro (Figure 1D), which showed Ipi-DM1 reduced viability of CLTA-4

expressing CHO but not wild type cells. As expected, there was no change in viability for either CHO cell lines when treated with Ipi (Figure 1D).

In order to evaluate the in vivo effects of CTLA-4 ADC on Tregs, we treated human CTLA-4 knock-in (Ctla4$^{h/h}$) mice with control hIgGFc or Ipi-DM1 ADC (Figure 1E). Peripheral blood was stained for flow cytometry and gated on CD45 and T-cell subset, including CD8, CD4, CD4 Foxp3^{+} and CD4 Foxp3^{-} subsets (Figure 1F). We found that Ipi-DM1 ADC significantly depleted Foxp3^{+} Tregs as indicated by the reduction in percentage and cell number of Foxp3^{+} CD4 T cells when compared to hIgGFc control (Figure 1G). In addition, total CTLA-4 levels and Ki67 staining in Tregs were decreased compared to control group (Figures 1H, 1I). In contrast, Ipi-DM1 ADC did not alter either % of CD4 Foxp3^{-} cells among CD45^{+} leukocytes or CTLA-4 levels on the subset, but did slightly decrease the cell number of CD4 Foxp3^{-} cells when compared hIgGFc control (Figure 1-figure supplement 1). Unexpectedly, Ipi-DM1 ADC caused a dramatic decline of B cells as percentages of CD45 and cell number in the periphery (Figure 1J). B cells from mice treated with Ipi-DM1 exhibited higher proliferation than those from hIgGFc treated control mice (Figure 1K).

Since a dramatic loss of B cells and a slight decrease in CD4-nonTregs in Ipi-DM1 treated mice were observed, we sought ensure that this phenomenon was not a result of downstream release of payload drug DM1. As shown in Figure 1-figure supplement 2A, hIgGFc-DM1 ADC (payload control) did not alter Treg percentage and cell number. A slightly higher level of CTLA-4 was noted in CD4 subset, while Treg proliferation did not change significantly compared to control (Figure 1-figure supplement 2B, 2C). No other effects on T cell subsets were noted (Figure 1-figure supplement 2D, 2E). Importantly, B cell number and proliferation were unaffected by hIgGFc-DM1 ADC treatment (Figure 1-figure supplement 2F, 2G).

Additionally, to ensure B cell depletion was not directly caused by Ipi-DM1 ADC, we stained $B220^+$ B cells and $Foxp3^+$ Tregs for human CTLA-4 in both human CTLA-4 knock-in ($Ctla4^{h/h}$) and WT mice to evaluate expression of CTLA-4 in B cells. As expected, CTLA-4 was detected in $Foxp3^+$ Tregs of $Ctla4^{h/h}$ but not B cells (Figure 1-figure supplement 3).

We then asked how Ipi-DM1 ADC induced Treg impairment impacted B cell lymphopoiesis. FACS analysis of bone marrow B cells revealed the loss of mature B cells but not immature transitional type1 or Pre-pro/Pro/Pre B cells from Ipi-DM1 treated mice, however the Pre-Pro/Pro/Pre B cell subtype percentage in B220 are enriched as a result of mature B cell loss (Figure 1L-1P, Figure 1-figure supplement 4). Additionally, CD21/35 expression level in the remaining mature B cells in Ipi-DM1 treated mice was lower than those from hIgGFc treated control mice (Figure 1Q). Taken together, data in Figure 1 showed that Ipi-DM1 can impair Treg function by depleting Tregs, preferentially the proliferating Tregs with higher CTLA-4 levels, and loss of B cells in the blood and bone marrow while B cell progenitors are not impacted.

B-cell depletion correlates with Treg impairment by Ipi-DM1

To investigate the kinetic relationship between the decline of B cells and Treg impairment, human CTLA-4 knock-in ($Ctla4^{h/h}$) mice were treated with control hIgGFc or Ipi-DM1 and bled according to schedule diagram in Figure 2A. We observed that peripheral blood samples from mice treated with Ipi-DM1 had a gradual decrease in total leukocytes compared hIgGFc control group followed by a full recovery by Day 25 (Figure 2B). The large decrease of CD45 cells in Ipi-DM1 group is predominantly attributed to the decline of B cells, which plateaus on days 9 and 13 and recovers by day 25 (Figures 2C, 2D) in correlation with the

kinetics of Tregs (Figure 2E, 2F). Similar to the bone marrow data in Figure 1, peripheral blood mature B cells decrease and transitional type1 B cells become enriched in Ipi-DM1 group compared hIgGFc control (Figure 2G-2I).

Depletion of T-cells but not macrophage rescues B-cells from ablation by Ipi-DM1

We then evaluated how Ipi-DM1-mediated impairment of Treg function affects total CD4 and CD8 T cells. Mice treated with Ipi-DM1 ADC did not affect the total percentage of CD4 or CD8 T cells among $CD45^{+}$ leukocytes, but the cell number of both cell types decreased (Figure 3A, 3B). Staining of Ki67 in CD4 and CD8 revealed a greater percentage of T cells in hyper-proliferative state (Figure 3C). Alternatively, mice treated with hIgGFc-DM1 did not change CD4 or CD8 percentage of CD45, cell numbers and Ki67 staining compared to hIgGFc control (Figure 3-figure supplement 1). We then analyzed the functional subsets of T cells in mice that received control hIgGFc or Ipi-DM1 at day 9. Using CD44 and CD62L markers, we observed an expansion of effector memory T cells ($CD44^{hi}CD62L^{low}$) in Ipi-DM1 group for both CD4 and CD8 T cells (Figures 3D, 3E). Correspondingly, the frequency of naive T cells was reduced for Ipi-DM1 while central memory T cells were unchanged (Figures 3D, 3E). These results show that CTLA-4 ADC can impair Treg function thereby resulting an increase in effector memory T cells and a hyper-proliferative state similar to animals that lack the expression of CTLA-4 or Foxp3.

Since B cells are devoid of CTLA-4, Ipi-DM1 must have induced other effector cells that are directly responsible for B cell depletion. To understand which cell types are responsible for the destruction of B cells, we depleted either T cells or macrophages using either anti-Thy1.2

mAb or chlondrosome. Ctla4$^{h/h}$ mice were treated with control hIgGFc, Ipi-DM1, Ipi-DM1 in combination with anti-Thy1.2, or Ipi-DM1 in combination with chlondrosome and bled on day 9 (Figure 4A). As shown in the Figure 4B, top panel, anti-Thy1.2 mAb efficiently depleted total T cells while macrophage depletion by chlondrosome had no effect (Figure 4B top panel, 4C, 4D). Additionally, combination of Ipi-DM1 with T cell depleting antibody resulted in a remarkable rescue of B cells as indicated by percentage B220 in CD45 and cell number while combination with macrophage depletion did not rescue the B cells (Figures 4B bottom panel, 4E).

In order to understand which subsets of T cells played a critical role in the T cell mediated destruction of B cells, we treated Ctla4$^{h/h}$ mice with hIgGFc control, Ipi-DM1, Ipi-DM1 with CD4 depleting antibody, or Ipi-DM1 with CD8 depleting antibody (Figure 4A). Both CD4 and CD8 depleting antibodies provide efficient depletion (Figure 4F, top panel) of their respective targeted T cell. Depletion of either CD4 or CD8 T cells results in B cell increase (Figures 4F bottom panel, 4I). Interestingly, the cell number of CD4 and CD8 T cells increase reciprocally by depletion of the other subsets (Figures 4G, 4H).

Taken together our CTLA-4 antibody-drug conjugate Ipi-DM1 can impair Treg function, which results in a T cell mediated destruction of B cells. Whole T cell depletion with anti-Thy1.2, depletion of CD4 or CD8 T cells rescued B cells from abrogation by Ipi-DM1.

B-cell rescue by Belatacept suggest a role for B7-CD28 interaction in B-cell depletion

The process for T cell activation requires two signals. The first signal is the binding of T-cell receptor (TCR) to antigen-bound major histocompatibility complex (MHC) and the second signal is a costimulatory molecule CD28 binding with B7-1/2 (CD80/86) on the antigen-

presenting cell. Having shown that the destruction of B cell can be prevented by total depletion of T cell, we sought to rescue the B cells by breaking the CD28-B7 signal with a soluble CTLA-4 that can bind to B7 but not Ipilimumab or Ipi-DM1 ADC. As shown in Figure 5-figure supplement 1, Abatacept can neutralize Ipilimumab/ADC while Belatacept does not. Therefore, Belatacept can be used to test if activation of T cells is required for B cell depletion.

We treated mice with Ipi-DM1 to impair Treg function and used Belatacept to break CD28/B7 signal to block T cell activation. Briefly, *Ctla4*$^{h/h}$ mice were treated with hIgGFc or Ipi-DM1 with/out Belatacept and bled on day 9 for flow analysis. Foxp3^{+} Tregs percentage in CD4 and cell number decreased similarly for Ipi-DM1 with/out Belatacept compared hIgGFc control (Figures 5A, 5B). Additionally, Belatacept did not impact Ipi-DM1 to target CTLA-4 expressing Tregs, as Ipi-DM1 with/out Belactacept had similar total CTLA-4 level reduction compared to control group (Figure 5C). However, Belatacept rescued B cells from Ipi-DM1-mediated depletion (Figures 5D, 5E). Correspondingly, Belatacept reduced effector memory T cells (Figures 5F, 5G) as well as granzyme B and IFN-γ expression in CD4 and CD8 T cells compared to Ipi-DM1 treated group (Figures 5H-5K, Figure 5-figure supplement 2).

Collectively, the data presented here show that Ipi-DM1 can impair Treg function resulting in T cell activation as indicated by increase in effector memory T cell markers, GranzymB, and cytokine production thereby resulting in the loss of B cells. However, under Ipi-DM1 induced Treg impairment the addition of mutant soluble CTLA-4-Ig, Belatacept, can reduce T cell activation and thereby preserving B cells.

B-cell depletion is partially rescued by anti-TNF-alpha

Since T cells are the effector cells responsible for B cell abrogation, it is of great interest to evaluate the molecular mechanism by which B cells are eliminated by T cells. To address this issue, we tested if either FasL or TNF-alpha, which are produced by activated T cells are responsible. To answer this question, Ctla4$^{h/h}$ mice were treated with hIgGFc control or Ipi-DM1 with/out Adalimumab a human anti-TNF-alpha that also binds to mouse TNF-alpha (Figure 6A, 6B). Flow analysis showed Tregs were decreased similarly between Ipi-DM1 with/out Adalimumab compared hIgGFc control group (Figures 6C top panel, 6D). Remarkably, the anti-TNF-alpha partially rescued B cells as shown by percentage difference of B cell marker B220 between Ipi-DM1 and in combination with Adalimumab as well as cell number (Figures 6C bottom panel, 6E). Peripheral blood samples stimulated with Iononmycin/PMA increased intracellular cytokines TNF-alpha and IFN-gamma for T cells from Ipi-DM1 treated mice compared to hIgGFc control, while that with Ipi-DM1 in combination with Adalimumab had slight increase but the change was insignificant except for IFN-gamma in CD8 T cells (Figure 6F, 6G). In contrast, blocking FAS-L with antibody did not result in B cell rescue (Figure 6-figure supplement 1).

DISCUSSION

We have reported that pH-insensitive anti-CTLA-4 antibodies trafficked to, and were degraded in the lysosomes.[23] Since lysosomal degradation is needed to release DM1 from the antibody for cytotoxicity, the pH-insensitive Ipilimumab was chosen for preparation of antibody-drug conjugate to be used to impact Treg function. We found that in Ctla4$^{h/h}$ mice anti-CTLA-4 ADC, Ipi-DM1, can recapitulate the phenotype of loss of B cells associated clinical deficiency of CTLA-4[8,9] /recycling partner LBRA[10]. Our analysis revealed B cell loss in both bone marrow

and peripheral blood, specifically mature B cells. Loss of mature peripheral B cells is consistent with clinical data for some patients with CTLA-4 haploinsufficiency.[8,9]

B cell loss was previously reported in mice with either naturally occurred (in Scurfy mice) or targeted mutation of Foxp3 and Treg depletion.[16-21]The kinetics of B cell loss and Treg depletion in the Ipi-DM1 treated mice revealed that B cell loss was transient and correlated to Treg impairment (proliferation, CTLA-4 level, cell number). Our data further showed that B cell destruction under Treg impairment conditions is T cell-mediated and required T cell activation.

Scurfy mice have poor central and peripheral B lymphopoiesis, however neonatal WT Treg adoptive transfer in scurfy mice resulted in robust population of mature B cells in the spleen.[19] Genetic ablation of TCRα gene by crossing scurfy with TCRA$\alpha^{-/-}$ mice efficiently support B cell lymphopoiesis and was sufficient to restore B cells in the bone marrow and peripheral compartments.[19] Additionally, reconstitution of bone marrow chimera from scurfy or wild type mixed with that from μMT mice that is deficient in B cells results in normal B cells after 8 weeks from reconstitution.[18] This is in line with our data that Treg impairment results in activated T-cells killing of B cells. Others have implied that under Treg depletion, activated T cells are targeting interleukin 7 (IL-7) secreting ICAM1+ perivascular stromal cells needed to progress B cell progenitors.[21] IL-7 is essential for B lymphopoiesis transition from Pro-B cell into Pre-B cell.[24] However, our model system is distinct where only mature B cells are depleted, while B cell progenitor precursors, and specifically Pre-B cells are not impacted. This suggest that activated T cells are directly responsible for B cell destruction. T cell activation initiated by Treg impairment requires B7-CD28 interaction for activated T cells. As a mechanism, we found that anti-TNF-alpha can partially rescue B-cells from loss imposed by Treg impairment.

While in vitro studies by others showed B cell killing by activated $CD25^{+}CD4$ Tregs, but not by $CD25^{-}$ CD4 T cells, [25] this is not the case in vivo where B cell loss is associated with Foxp3 Treg loss or impairment. [16-21] Furthermore, our current study shows that both CD4 and CD8 T cells contributed to B cell loss. The concept that B cells are actively eliminated by T cells in vivo expands our understanding of T-B cell interaction by showing antagonism rather than just "immunological help" from T cells to B cells.

MATERIALS and METHODS

Experimental animals

C57BL/6 mice that express the CTLA-4 protein with 100% identity to human CTLA-4 protein under the control of endogenous mouse *Ctla4* locus, *Ctla4*$^{h/h}$, have been previously described.[26] All animals used in experiments were 7-9 weeks age (female mice were used unless male mice are indicated). No blinding or randomization was used and mice were fairly distributed into different treatment groups so that initial average weight of each group were similar. All mice were maintained at the Research Animal Facility of the Institute of Human Virology at the University of Maryland Baltimore School of Medicine. All animal studies were approved by the Institutional Animal Care and Use Committee.

Cell culture and treatment

CHO cells that were stably transfected with human CTLA-4 have been reported.[27] CHO cells were grown in DMEM (Dulbecco's Modified Eagle Medium, Gibco) supplemented with 10% FBS (Hyclone), 100 units/mL of penicillin and 100 μg/mL of streptomycin (Gibco). Mice Peripheral blood leukocytes were cultured in RPMI-1640 medium (containing 10% FBS and 2%

penicillin/streptomycin). All cell lines were incubated at 37 °C and were maintained in an atmosphere containing 5% CO2.

Viability assay

Wild type CHO (CHO-WT) or human CTLA-4 expressing CHO (CHO-hCTLA-4) cells were seeded at 1,000 cell/well in a flat 96-well plate at 37 °C for 24 hrs in cell culture incubator. The medium was then replaced with fresh medium containing 1/4 serially diluted vehicle (PBS), Ipilimumab or Ipilimumab-DM1 ADC and cell were incubated at 37 °C for additional 72 hrs. Each treatment group was in duplicate or triplicates. CCK-8 viability dye was then added to each well according to manufacturer's protcol and incubated for another (2-2.5 hrs) at 37 °C. Wells were subsequently read for absorbance at 450nM on Spectramax ID3 Molecular Devices plate reader. In case of testing whether soluble human CTLA-4-Ig or mutant can neutralize Ipilimumab or Ipilimumab-DM1, the same conditions above were used except that Abetacept or Belatacept concentrations were kept constant at 6 μg/mL. Data is normalized according to the following equation ($treatment_{OD450}$ - $background_{averageOD450}$ /$vehicle_{averageOD450}$ - $background_{average}$) x 100.

Cell surface CTLA-4 binding

Freshly trypsinized human CTLA-4 expressing CHO (CHO-hCTLA-4) cells were stained with 1/4 serially dilute anti-CTLA-4 Iplimiumab or Iplimiumab-DM1 ADC in FACS buffer (2% FBS with 2 mM EDTA) for 30 minutes on ice. Cells were then washed twice with FACS buffer and incubated with anti-human IgG AF488 secondary antibody for 20 minutes on ice. Cells were washed twice with FACS buffer and processed on BD Canto II flow cytometer. In the case of

whether soluble human CTLA-4-Ig or mutant can neutralize Ipilimumab or Ipilimumab-DM1 and prevent them from binding cell to surface CTLA-4 the same conditions above were used except that Abetacept or Belatacept concentrations were kept constant at 6 μg/mL.

Peripheral blood T cell stimulation

Peripheral blood samples 50 μL were treated with ACK Lysis buffer and washed with RPMI-1640 medium. Leukocytes were then stimulated with 1 μg/ml each of phorbol 12-myristate 13-acetate (PMA) (Sigma-Aldrich, St. Louis, MO), ionomycin (Sigma Aldrich, St. Louis, MO) and BD GolgiStop™ (BD Biosciences, cat. 51-2092KZ) and cultured in RPMI-1640 medium (containing 10% FBS and 2% penicillin/streptomycin) for 4 hours at 37°C in 96-well plate. Medium was removed and cells were washed twice with FACS buffer (2% FBS with 2 mM EDTA) followed by surface staining and fix/perm and intracellular staining.

Flow Cytometry

Leukocytes from blood or bone marrow were FACS stained directly or after red blood cell lysis with ACK buffer. Fc Receptor was blocked with anti-FCR clone 2.4G2 at 10 μg/mL in FACS buffer for 10 minutes at room temperature and respective surface staining antibodies cocktails were added to each sample and incubated on ice for additional 20 minutes. Cells were then washed twice with 1xPBS and stained with 1x live/Dead Fixable dye Aqua in 1x PBS for 7 minutes at room temperature. Cells were then washed twice with FACS buffer and fixed with eBioscience™ Foxp3/Transcription Factor Staining Buffer Set for 40 minutes. Samples were either washed twice and resuspended in FACS buffer and processed for flow acquisition or further permeabilized for intracellular staining using perm buffer from same kit (eBioscience™ Foxp3/Transcription Factor Staining Buffer Set). In General, all intracellular staining of Foxp3, Ki67, hCTLA-4, GranzymeB,

or cytokines were done overnight at 4 degree. In the case of detecting intracellular cytokines, samples were cultured and simulated according to the above protocol followed by surface then intracellular cytokine staining. Samples were acquired by the BD Canto II Flow cytometer and data were analyzed by Flowjo software.

ELISAs

96-well high-binding polystyrene plates were pre-coated with 50 μL of 1 μg/mL of His-hCTLA-4, or mouse TNF-alpha in coating buffer (0.1M bicarbonate) at 4°C overnight. After washing away the unbound protein/antibody thrice with 0.05% PBST, the plates were blocked with blocking buffer (1% BSA in PBST) for 1hr at room temperature. All primary antibody incubation was done in blocking buffer at 4°C overnight or room temperature for 1 hour. For coated His-hCTLA-4 a given concentration of either Ipilimumab/DM1, or hIgGFc/DM1; For coated mouse TNF-alpha a given concentration of Adalimumab or Ipilimumab negative control were used. Following primary incubation plates were then washed with PBST for four times and incubated with a goat anti-human IgGFc HRP conjugate secondary antibody at 1/20,000 dilution for detection in blocking buffer for 1 hr at room temperature. Plates were then washed 4 times with PBST followed by development with 1-Step™ Ultra TMB-ELISA Substrate Solution for 10 minutes and stopped with 2N sulfuric acid. Wells were read at 450nM on Spectramax ID3 Molecular Devices plate reader.

Antibody-drug conjugate preparation

Ipilimumab or hIgGFc were buffer exchanged using prepacked column PD-10 into 1X PBS. Ipilimumab or hIgGFc 5 mg each at concentration 1.5 mg/mL were conjugated with SMCC-DM1(15 eq) in 1x PBS in the presence of 10% DMSO at 37°C under mild shaking conditions

for 50 minutes to furnish Ipilimumab-DM1 or hIgGFc-DM1 ADC respectively. Reaction mixture was cleaned up from excess SMCC-DM1 by buffer exchange with a in house ADC buffer at pH 6.5 containing (20 mM Histidine, 8 % sucrose, and Polysorbate 80 0.02%) by Econo-Pac 10DG prepacked column according to manufacturer protocol. Confirmed fraction containing ADC by nano drop were combined and concentrated down to 1 mL using Pierce™ Protein Concentrator PES, (30K for hIgGFc-DM1) or (50K for Ipilimumab-DM1) MWCO according manufacture protocol followed by sterile filtration. ADC concentration was determined using BCA assay according to manufacturer protocol. ADC were diluted to 0.4 – 0.5 mg/mL in 1xPBS and A_{280} &A_{252} were recorded on Nanodrop One. The drug to antibody ratio (DAR) was calculated following previous literature.[28]

Antibodies and fusion proteins used for in vivo studies

CTLA-4-Ig fusion proteins were synthesized by Sydlabs, Inc (Boston, MA). Recombinant Ipilimumab with amino acid sequence disclosed in WC500109302 was produced by Sydlabs Inc. (Boston, MA). Azide-free human IgG-Fc was purchased from Athens Research and Technology (Athens, GA, USA). Antibody-drug conjugates Ipilimumab-DM1 and hIgGFc-DM1 were prepared from parent antibodies in lab. Depletion antibodies anti-mouse Thy1.2, clone 30H12(BE0066); anti-mouse CD4, clone GK1.5 (BE0003-1); and anti-mouse CD8α, clone 2.43 (BE00-61) were purchased by Bioxcell Inc. (West Lebanon, NH, USA). Anti-mouse FASL, clone MFL3 (BE00319) was purchased by Bioxcell Inc. (West Lebanon, NH, USA). Anti-TNF-α, Adalimumab, clinical grade Humira™ was purchased from Premium Health Services (Columbia, MD, USA).

Other reagents and material

SMCC-DM1 drug payload with cross linker (Cederlanelabs/Cayman Chemical Co, 23926-10) Anti-mouse FcγR, clone 2.4G2 (Bioxcell Inc, BE0307). Clodrosome® (Encapsula Nano Sciences, SKU# CLD-8909). Mouse anti-human IgGFc secondary antibody (Invitrogen/Thermo Fisher Scientific, 05-42-00). Goat anti-human IgGFc (HRP) preadsorbed (Abcam, ab98624). Polyhistidine-tagged human CTLA-4 (HIS-hCTLA-4) (Sino Biological Inc, 11159-H08H). Mouse TNF-alpha (Sino Biological Inc, 50349-MNAE). 123 eBeads™ counting beads flow (Thermo Fisher Scientific/Invitrogen, 01-1234-42). NuPage™ BIS-TRIS gels 4-12% (Thermo Fisher Scientific/Invitrogen, NP0335BOX). NuPAGE™ MOPS SDS Running Buffer (20X) (Thermo Fisher Scientific/Invitrogen, NP0001). NuPage™ LDS sample buffer (4x) (Thermo Fisher Scientific/Invitrogen, NP0007). Protein Ladder (Fisher Scientific, BP3603500). Sucrose (Sigma Aldrich, S0389-1KG). L-Histidine (Sigma Aldrich, H8000-10G). Dimethyl sulfoxide (DMSO) (Santa Cruz Biotechnology, Sc-258801). Polysorbate 80 (Fisher Scientific, L13315). Buffer exchange prepacked column PD-10 (GE health care/ Cytiva Life Sciences, 17085101). Buffer exchange prepacked column Econo-Pac 10DG (Bio-Rad, 7322010). Cell Counting Kit-8 (CCK-8) (Bimake, B34304). 1-Step™ Ultra TMB-ELISA Substrate Solution (Thermo Fisher Scientific, 34028). Gibco™ ACK Lysing buffer (Thermo Fisher scientific/Gibco, A1049201). Live/Dead™ Fixable Aqua Dead Cell Stain (Thermo Fisher Scientific/Life Technologies, L34966). eBioscience™ Foxp3 / Transcription Factor Staining Buffer Set (Thermo Fisher Scientific/Invitrogen, 00-5523-00). Pierce™ Protein Concentrator PES, 30K MWCO, 2-6 mL (Thermo Fisher Scientific/ Pierce, 88521) Pierce™ Protein Concentrators PES, 50K MWCO, 2–6 mL (Thermo Fisher Scientific/ Pierce, 88538). Pierce™ BCA Protein Assay Kit (Thermo Fisher Scientific/Pierce, 23227).

Flow antibodies

eBioscience/ Thermo Fisher Scientific (San Diego, CA): APC-eFlour780 anti- mouse CD45, clone 30-F11 (47-0451-82);eFlour450 anti-mouse CD4, clone GK1.5 (48-0041-82); Pacific Blue anti-mouse CD4, clone RM-4-4 (116008); PE-Cyanine7 anti-mouse CD8α, clone 53-6.7 (25-0081-82); PE-Cyanine7 anti-mouse CD8β, clone H35-17.2 (25-0083-82);PerCP-Cy5.5 anti-mouse B220, clone RA3-6B2 (45-0452-82); APC anti-mouse Foxp3, clone FJK-16s (17-5773-82);FITC anti-mouse Ki67, clone SolA15 (11-5698-82);FITC Isotype rat IgG2ak, clone eBR2a (11-4321-82);FITC anti- mouse CD44, clone IM7 (11-0441-85);PerCP-Cy5.5 anti-mouse CD62L, clone MEL-14 (45-0621-82);PE-Cyanine7 anti-mouse B220, clone RA3-6B2 (25-0452-82); APC anti-mouse IgM, clone II/41 (17-5790-82); eFlour 450 anti-mouse CD21/CD35, clone 4E3 (48-0212-82); AF488 anti-mouse TNF-α, clone MP6-XT22 (53-7321-82);AF488 Isotype rat IgG1k, clone eBRG1 (53-4301-80); APC anti-mouse IFNγ, clone XMG1.2 (17-7311-82);APC Isotype rat IgG1k, clone eBRG1 (17-4301-82);FITC anti- mouse GranzymeB, clone NGZB (11-8898-82); Alexa Fluor 488-conjugated goat anti-human IgG (H+L) cross-adsorbed secondary antibody (A-11013). BioLegend (San Diego, CA): PE anti-human CTLA-4, clone BNI3 (369604);PE Isotype mIgG2ak, clone MPC-173 (400212); PerCP-Cy5.5 anti-mouse IgD, clone 11-26c.21 (405710); BV421 anti-mouse CD21/CD35, clone 7E9 (12342);

Statistical analysis

The specific tests used to analyze each set of experiments are indicated in the figure legends. Data were analyzed using a two-tailed t-test to compare between two groups or by one-way ANOVA (analysis of variance) for multiple comparisons. In the graphs, y-axis error bars

represent S.E.M. or S.D. as indicated. Statistical calculations were performed using GraphPad Prism software (GraphPad Software, San Diego, California). *$p < 0.05$, **$p < 0.01$, ***$p < 0.001$, ****$p < 0.0001$. Reported CTLA-4 level and absolute cell numbers are normalized by the average value of hIgGFc control group.

Acknowledgments

Funding: This study is supported by grants from the National Institutes of Health (R01AI154722) and OncoC4, Inc.

Author contributions: M.M.M performed the study with technical assistance from X.D. M.L., X.W., W.W., and C.A.; M.M.M, Y.L, P.Z, and L.S. designed and/or supervised the research. M.M.M and Y.L. wrote the paper with input from other coauthors.

Competing interests: All authors declare no competing interests**.**

Data and materials availability: All data are available in the main text or the supplementary materials.

Supplementary Materials

Table S1. Drug to antibody ratio (DAR)

Figure 1-figure supplement 1. CD4-nonTregs and CTLA-4 expression

Figure 1-figure supplement 2. B-cell depletion is not mediated by DM1 payload off-target release

Figure 1-figure supplement 3. B-cells do not express CTLA-4

Figure 1-figure supplement 4. IgM negative B-cell subtypes in bone marrow

Figure 3-figure supplement 1. T-cell quantity and proliferation are not impacted by IgG-DM1 treatment

Figure 5-figure supplement 1. Mutant soluble CTLA-4-Ig does not neutralize Ipilimumab or its drug conjugate

Figure 5-figure supplement 2. T-cell cytokine production

Figure 6-figure supplement 1. Anti-FASL fails to rescue B cells

References

1. Bennett CL, Christie J, Ramsdell F, et al. The immune dysregulation, polyendocrinopathy, enteropathy, X-linked syndrome (IPEX) is caused by mutations of FOXP3. *Nature Genetics.* 2001;27(1):20-21.
2. Brunkow ME, Jeffery EW, Hjerrild KA, et al. Disruption of a new forkhead/winged-helix protein, scurfin, results in the fatal lymphoproliferative disorder of the scurfy mouse. *Nature Genetics.* 2001;27(1):68-73.
3. Fontenot JD, Gavin MA, Rudensky AY. Foxp3 programs the development and function of CD4+CD25+ regulatory T cells. *Nature Immunology.* 2003;4(4):330-336.
4. Wildin RS, Ramsdell F, Peake J, et al. X-linked neonatal diabetes mellitus, enteropathy and endocrinopathy syndrome is the human equivalent of mouse scurfy. *Nature Genetics.* 2001;27(1):18-20.
5. Wildin RS, Smyk-Pearson S, Filipovich AH. Clinical and molecular features of the immunodysregulation, polyendocrinopathy, enteropathy, X linked (IPEX) syndrome. *Journal of Medical Genetics.* 2002;39(8):537-545.
6. Tivol EA, Borriello F, Schweitzer AN, Lynch WP, Bluestone JA, Sharpe AH. Loss of CTLA-4 leads to massive lymphoproliferation and fatal multiorgan tissue destruction, revealing a critical negative regulatory role of CTLA-4. *Immunity.* 1995;3(5):541-547.
7. Waterhouse P, Penninger JM, Timms E, et al. Lymphoproliferative Disorders with Early Lethality in Mice Deficient in Ctla-4. *Science.* 1995;270(5238):985-988.
8. Kuehn HS, Ouyang W, Lo B, et al. Immune dysregulation in human subjects with heterozygous germline mutations in CTLA4. *Science.* 2014;345(6204):1623-1627.
9. Schubert D, Bode C, Kenefeck R, et al. Autosomal dominant immune dysregulation syndrome in humans with CTLA4 mutations. *Nature Medicine.* 2014;20(12):1410-1416.
10. Lo B, Zhang K, Lu W, et al. Patients with LRBA deficiency show CTLA4 loss and immune dysregulation responsive to abatacept therapy. *Science.* 2015;349(6246):436-440.
11. Wing K, Onishi Y, Prieto-Martin P, et al. CTLA-4 Control over Foxp3⁺ Regulatory T Cell Function. *Science.* 2008;322(5899):271-275.
12. Wing James B, Ise W, Kurosaki T, Sakaguchi S. Regulatory T Cells Control Antigen-Specific Expansion of Tfh Cell Number and Humoral Immune Responses via the Coreceptor CTLA-4. *Immunity.* 2014;41(6):1013-1025.

478 13. Sage Peter T, Paterson Alison M, Lovitch Scott B, Sharpe Arlene H. The Coinhibitory Receptor
479 CTLA-4 Controls B Cell Responses by Modulating T Follicular Helper, T Follicular Regulatory, and
480 T Regulatory Cells. *Immunity.* 2014;41(6):1026-1039.
481 14. Klocke K, Sakaguchi S, Holmdahl R, Wing K. Induction of autoimmune disease by deletion of
482 CTLA-4 in mice in adulthood. *Proceedings of the National Academy of Sciences.*
483 2016;113(17):E2383-E2392.
484 15. Leonardo SM, De Santis JL, Gehrand A, Malherbe LP, Gauld SB. Expansion of follicular helper T
485 cells in the absence of Treg cells: Implications for loss of B-cell anergy. *European Journal of*
486 *Immunology.* 2012;42(10):2597-2607.
487 16. Clark LB, Appleby MW, Brunkow ME, Wilkinson JE, Ziegler SF, Ramsdell F. Cellular and Molecular
488 Characterization of the scurfy Mouse Mutant. *The Journal of Immunology.*
489 1999;162(5):2546-2554.
490 17. Chen C, Liu Y, Liu Y, Zheng P. Mammalian target of rapamycin activation underlies HSC defects in
491 autoimmune disease and inflammation in mice. *The Journal of Clinical Investigation.*
492 2010;120(11):4091-4101.
493 18. Chang S-E, Guo L, Tian J, et al. Autoimmune bone marrow environment severely inhibits B cell
494 development by inducing extensive cell death and inhibiting proliferation. *Autoimmunity.*
495 2012;45(3):210-217.
496 19. Riewaldt J, Düber S, Boernert M, et al. Severe Developmental B Lymphopoietic Defects in Foxp3-
497 Deficient Mice are Refractory to Adoptive Regulatory T Cell Therapy. *Frontiers in Immunology.*
498 2012;3.
499 20. Leonardo SM, Josephson JA, Hartog NL, Gauld SB. Altered B Cell Development and Anergy in the
500 Absence of Foxp3. *The Journal of Immunology.* 2010;185(4):2147-2156.
501 21. Pierini A, Nishikii H, Baker J, et al. Foxp3+ regulatory T cells maintain the bone marrow
502 microenvironment for B cell lymphopoiesis. *Nature Communications.* 2017;8(1):15068.
503 22. Das R, Bar N, Ferreira M, et al. Early B cell changes predict autoimmunity following combination
504 immune checkpoint blockade. *The Journal of Clinical Investigation.* 2018;128(2):715-720.
505 23. Zhang Y, Du X, Liu M, et al. Hijacking antibody-induced CTLA-4 lysosomal degradation for safer
506 and more effective cancer immunotherapy. *Cell Research.* 2019;29(8):609-627.
507 24. von Freeden-Jeffry U, Vieira P, Lucian LA, McNeil T, Burdach SE, Murray R. Lymphopenia in
508 interleukin (IL)-7 gene-deleted mice identifies IL-7 as a nonredundant cytokine. *Journal of*
509 *Experimental Medicine.* 1995;181(4):1519-1526.
510 25. Zhao D-M, Thornton AM, DiPaolo RJ, Shevach EM. Activated CD4+CD25+ T cells selectively kill B
511 lymphocytes. *Blood.* 2006;107(10):3925-3932.
512 26. Lute KD, May KF, Jr., Lu P, et al. Human CTLA4 knock-in mice unravel the quantitative link
513 between tumor immunity and autoimmunity induced by anti-CTLA-4 antibodies. *Blood.*
514 2005;106(9):3127-3133.
515 27. Du X, Tang F, Liu M, et al. A reappraisal of CTLA-4 checkpoint blockade in cancer
516 immunotherapy. *Cell Res.* 2018;28(4):416-432.
517 28. Chen Y. Drug-to-Antibody Ratio (DAR) by UV/Vis Spectroscopy. In: Ducry L, ed. *Antibody-Drug*
518 *Conjugates.* Totowa, NJ: Humana Press; 2013:267-273.

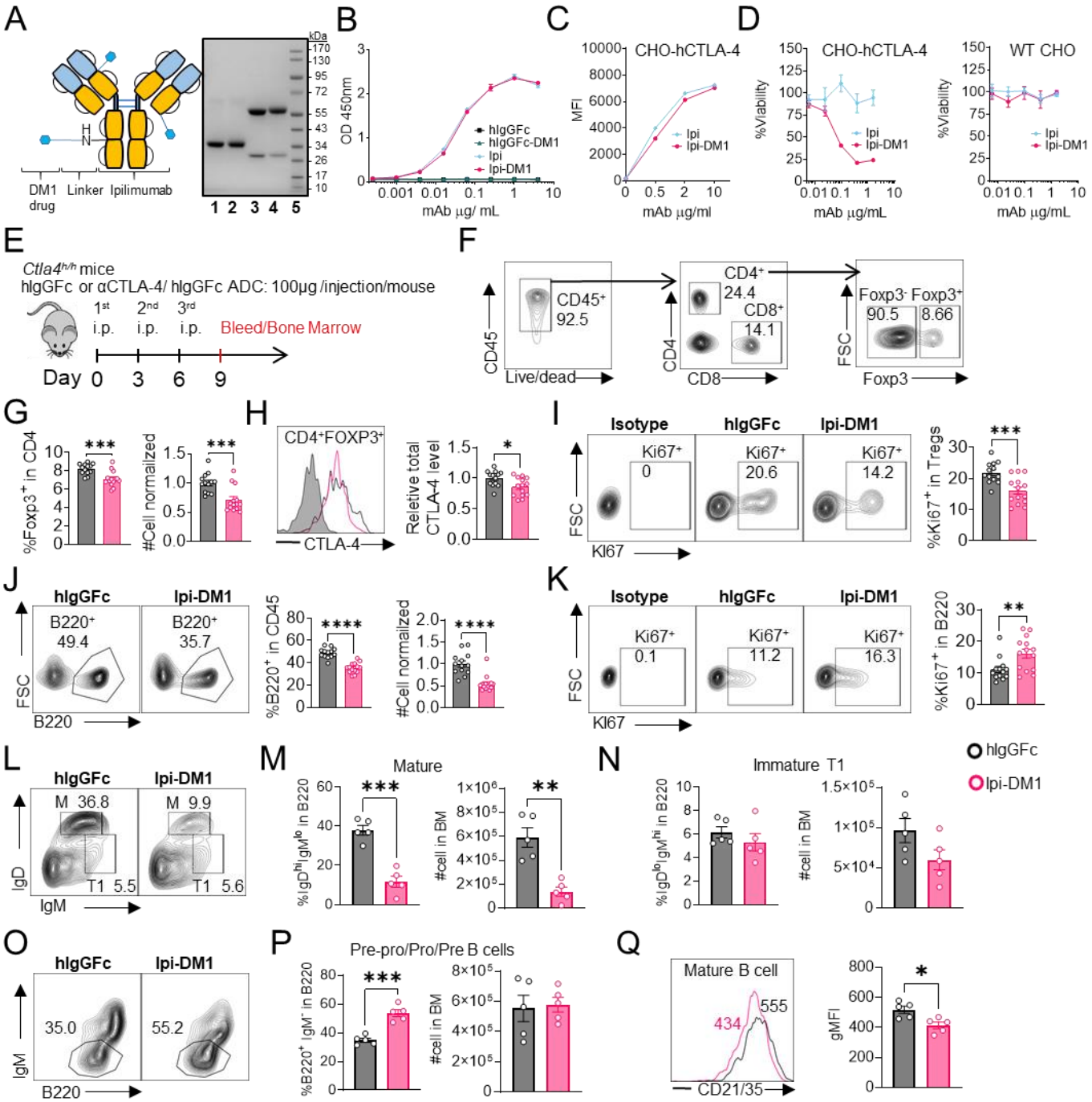

519

520 **Figure 1. CTLA-4 antibody-drug conjugate impairs regulatory T-cell and leads to B-cell**

521 **depletion.**

522 (A) SDS-Reducing gel showing size shift after DM1 conjugation. Lanes (left to right) are 1

523 hIgGFc, 2 hIgGFc-DM1 antibody-drug conjugate (ADC), 3 Ipilimumab (Ipi), 4 Ipilimumab-

524 DM1 (Ipi-DM1) antibody-drug conjugate (ADC), and 5 Ladder. (B) ELISA binding of hIgGFc,
525 hIgGFc-DM1, Ipi, and Ipi-DM1 to pre-coated 1 μg/mL His-hCTLA-4 and detected with anti-
526 hIgG-HRP (n=2). (C) Flow cytometry binding of Ipi and Ipi-DM1 to hCTLA-4 expressing CHO
527 cells (CHO-hCTLA-4) and detected with anti-hIgG-AF488. (D) Cell viability of CHO-hCTLA-4
528 cells and wild type CHO cells after 72 hours incubation with Ipi or Ipi-DM1 as measured by
529 MTT assay (n=2). (E) Diagram of experimental design, *Ctla4*$^{h/h}$ mice were treated
530 intraperitoneally (i.p.) (100 μg/mouse) with hIgGFc or Ipi-DM1 every three days and mice were
531 bled or harvested for bone marrow extraction on day 9 for downstream flow analysis. (F-K) Flow
532 data analysis of day 9 peripheral blood. (F) Gating strategy defining T-cell types, Tregs (CD4^{+}
533 Foxp3^{+}) and CD4-nonTreg (CD4^{+} Foxp3^{-}). (G) % Foxp3^{+} in CD4 and normalized cell number.
534 (H) Relative CTLA-4 Level in Tregs. (I) % Ki67^{+} in Tregs. (J) FACS profile of B cells defined
535 (CD45^{+} B220^{+}) and data summaries of % B220^{+} in CD45 and normalized cell number. (K) %
536 Ki67^{+} in B cells. (L-Q) flow data analysis of day 9 bone marrow after gating on CD45^{+}B220^{+},
537 mature (M) (IgD^{hi} IgM^{low}), immature transitional type 1 (T1) (IgD^{low}IgM^{+}), and Pre-pro/Pro/Pre
538 B cell subtypes (B220^{+}IgM^{-}). (L) FACS profile gating, (M) % of mature B cells in B220 and
539 absolute cell number summaries, (N) % of T1 immature B cells in B220 and absolute cell
540 number summaries. (O) FACS profile gating of Pre-pro/Pro/Pre B cells, (P) % of Pre-pro/Pro/Pre
541 B cells in B220 and absolute cell number summaries. (Q) CD21/35 expression in mature B cells
542 in bone marrow. (B-D) representative data two or more repeats. (F-K) Data combined from two
543 independent experiments (n=13-14). (L-Q) Data representative of two independent experiments
544 (n=5). Data analyzed using an unpaired two-tailed Student's t test and represented as mean ±
545 SEM. *$p < 0.05$, **$p < 0.01$, ***$p < 0.001$, ****$p < 0.0001$.

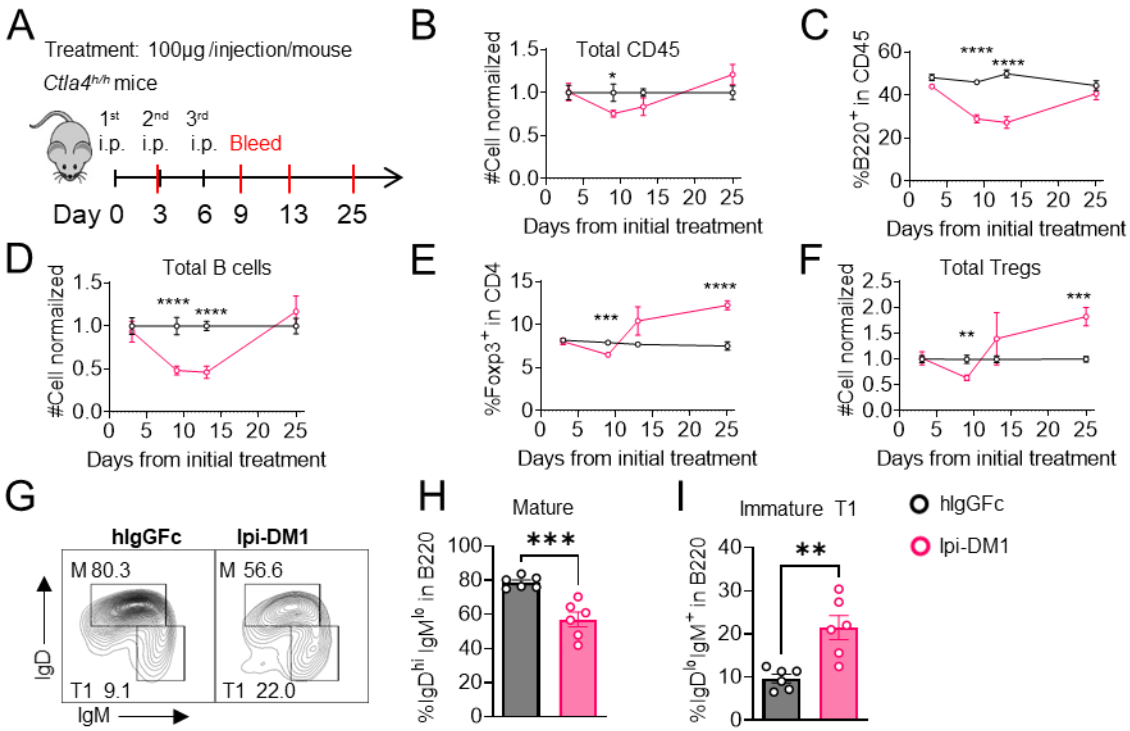

Figure 2. B-cell depletion is transient and correlated with a decrease in regulatory T-cell.

(A) Diagram of experimental design, *Ctla4*$^{h/h}$ mice were treated intraperitoneal (i.p.) (100 µg/mouse) with hIgGFc or Ipi-DM1 every three days and mice were bled on day 3,9,13, 25 for downstream flow analysis. (B-F) Flow data of time course of CD45, B, and Treg cells in peripheral blood, (B) CD45 normalized cell number, (C) % of B-cells in CD45, (D) B-cell normalized cell number, (E) % Foxp3^{+} Tregs in CD4, (F) Treg normalized cell number. (G-J) Flow analysis of B-cell subtypes from day 13 peripheral blood. (G) FACS profile of Mature (M) (IgD^{hi} IgM^{low}), and immature Transitional type 1 (T1) (IgD^{low} IgM^{+}) B cell subtypes after gating on CD45^{+}B220^{+} B cells. (H) % of mature B cells in B220. (I) % of T1 B cells in B220. (B-F) Data is combined from two independent experiments (n=10). (G-I) Data is representative of two independent experiments (n=6). Data were analyzed by an unpaired two-tailed Student's t test and represented as mean ± SEM. *$p < 0.05$, **$p < 0.01$, ***$p < 0.001$, ****$p < 0.0001$

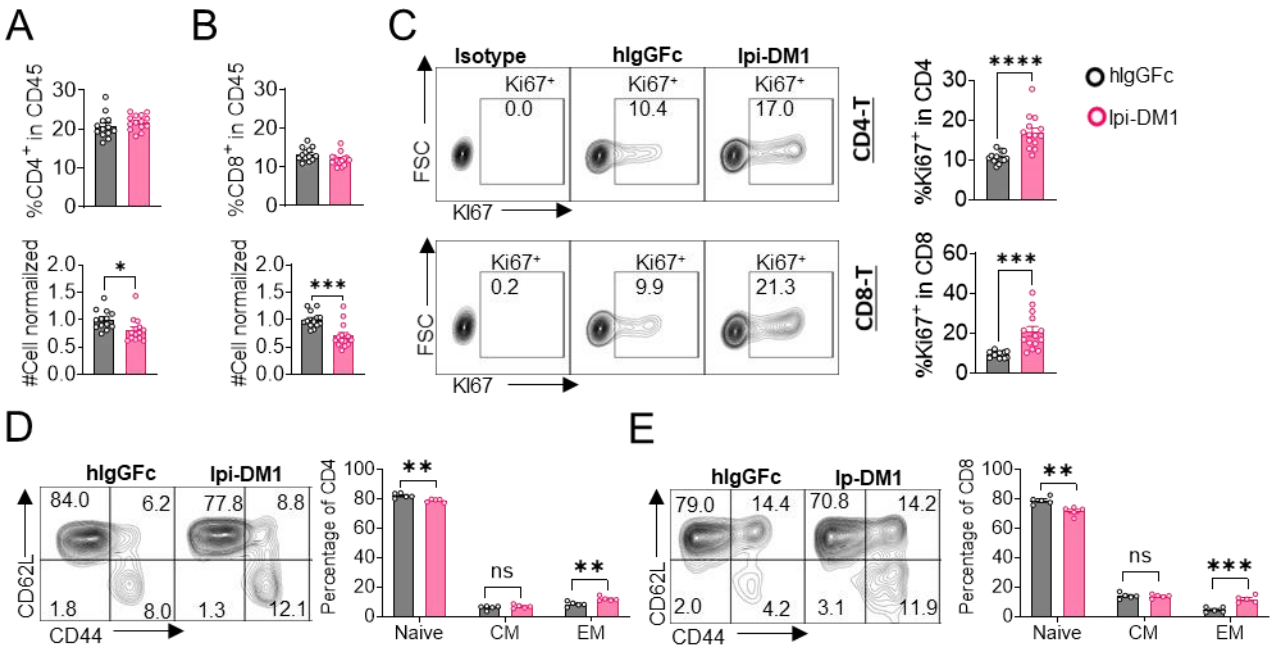

Figure 3. CTLA-4 antibody-drug conjugate leads to T-cell activation.

Flow data analysis of peripheral blood from *Ctla4*$^{h/h}$ mice on day 9 after treatment with hIgGFc or ADC (hIgGFc-DM1 or Ipi-DM1). (A) % CD4^{+} in CD45 and normalized cell number. (B) % CD8^{+} in CD45 and normalized cell number. (C) % Ki67^{+} in CD4 and CD8 T cells. (D, E) FACS profiles and summaries depicting the increase in effector T-cells after Ipi-DM1 treatment, naïve (Q1: CD44^{low} CD62L^{hi}), central memory (Q2: CD44^{hi} CD62L^{hi}) and effector (Q3: CD44^{hi} CD62L^{low}), (D) phenotype of CD4^{+} T cells (E), and CD8^{+} T cells (H). (B-C) Mice treated with hIgGFc or Ipi-DM1, data combined from two independent experiments (n=13-14). (D-E) Mice treated with hIgGFc or Ipi-DM1, data is representative of two independent experiments (n=5). Data analyzed using an unpaired two-tailed Student's t test and represented as mean ± SEM. Non-significant [ns], *$p < 0.05$, **$p < 0.01$, ***$p < 0.001$, ****$p < 0.0001$.

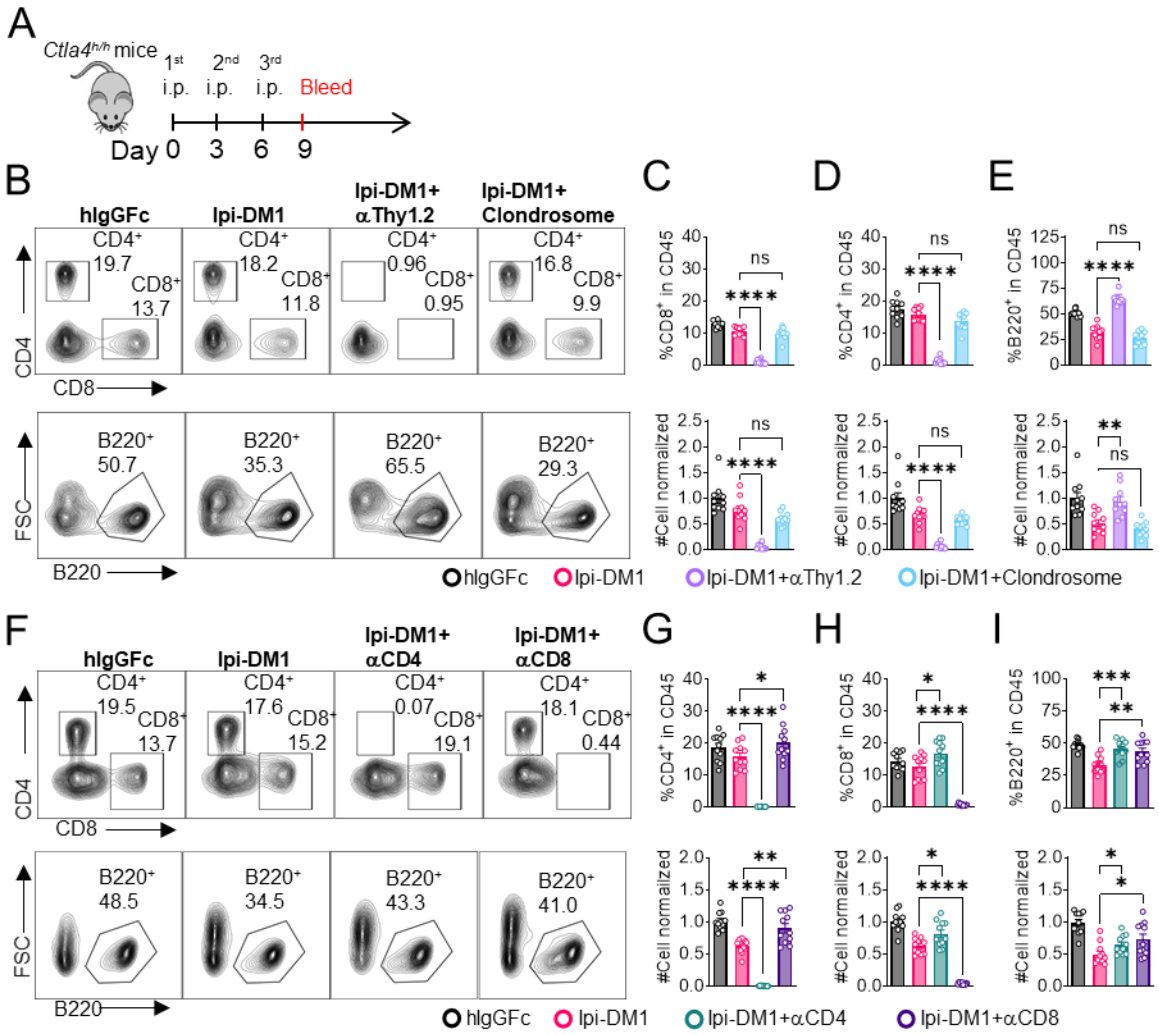

Figure 4. B-cell depletion depends on T-cells but not macrophage.

(A) Diagram of experimental design, male or female *Ctla4*$^{h/h}$ mice were treated intraperitoneal (i.p.) (100 µg/mouse) with hIgGFc or Ipi-DM1 with/out (T-cell depleting antibody 100 µg/mouse of anti-Thy1.2 or 150µL/mouse of clondrosome or depleting antibody CD4 or CD8 100 µg/mouse) every three days and mice were bled on day 9 for downstream flow analysis. (B) FACS profiles depicting gating strategy after gating on CD45 for CD8 & CD4 T (top panel) and B cells (bottom panel). (C-E) Data summaries from FACS profile(panel B), (C) % CD4^{+} in CD45 and normalized cell number, (D) % CD8^{+} in CD45 and normalized cell number, and (E) % B220^{+}

580 in CD45 and normalized cell number. (F) FACS profiles depicting gating strategy after gating on
581 CD45 for CD8 & CD4 T (top panel) and B cells (bottom panel). (G-I) Data summaries from
582 FACS profile(panel F), (G) % $CD4^+$ in CD45 and normalized cell number, (H) % $CD8^+$ in CD45
583 and normalized cell number, and (I) % $B220^+$ in CD45 and normalized cell number. (B-E) Data
584 combined from two independent experiments (n=10) and analyzed by ordinary one-way ANOVA
585 with Tukey's multiple comparisons test and represented as mean ± SEM. Non-significant [ns],
586 *$p < 0.05$, **$p < 0.01$, ***$p < 0.001$, ****$p < 0.0001$. (F-I) Data combined from two independent
587 experiments (n=11) and analyzed by unpaired two-tailed Student's t test and represented as mean
588 ± SEM. Non-significant [ns], *$p < 0.05$, **$p < 0.01$, ***$p < 0.001$, ****$p < 0.0001$.

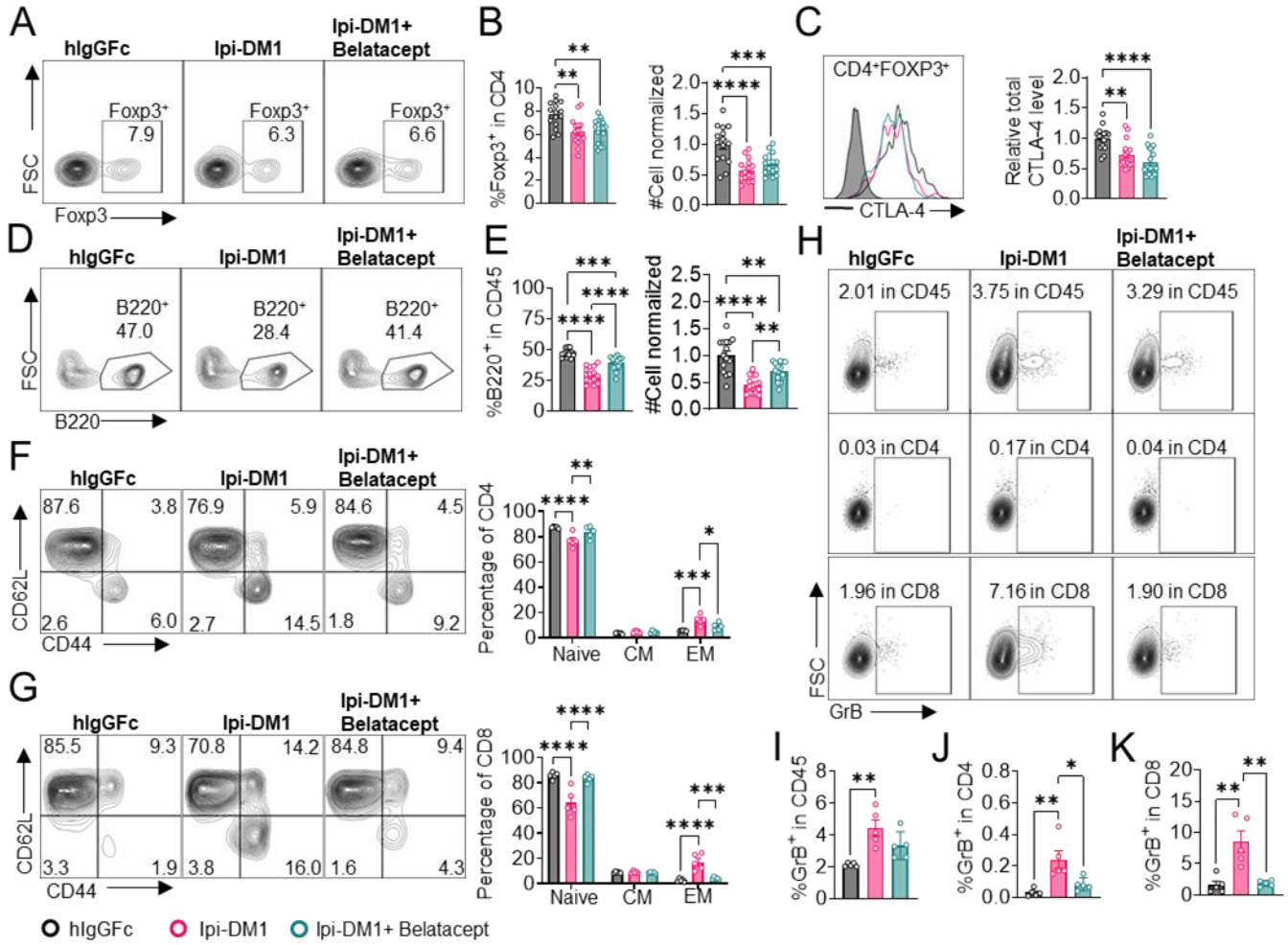

Figure 5. Mutant soluble CTLA-4-Ig rescues B-cell.

Ctla4$^{h/h}$ mice were treated intraperitoneal (i.p.) (100 µg/mouse) with hIgGFc or Ipi-DM1 with/out (100 µg/mouse of Belatacept) every three days for total of three doses and mice were bled on day 9 for downstream flow analysis.(A, D) FACS profiles depicting gating strategy after gating on CD45 for (A) Tregs (% Foxp3^{+} in CD4 T cells) and (D) B cells (% B220^{+} in CD45). (B) % Foxp3^{+} (Tregs) in CD4 and normalized cell number. (C) Representative FACS profile of CTLA-4 expression in Tregs (CD4^{+} Foxp3^{+}) and Relative CTLA-4 summary. (E) % B220^{+} in CD45 and normalized cell number. (F-G) FACS gate and summaries showing mutant CTLA-4-Ig can decrease effector memory T-cells associated with Ipi-DM1 treatment, naïve (Q1: CD44^{low}

599 $CD62L^{hi}$), central memory (Q2: $CD44^{hi}$ $CD62L^{hi}$) and effector (Q3: $CD44^{hi}$ $CD62L^{low}$),

600 phenotype of $CD4^{+}$ T cells (F), and $CD8^{+}$ T cells (G). (H) FACS of GranzymeB gating in CD45

601 (Top panel), CD4 (middle panel), and CD8 (bottom panel). (I-K) GranzymeB expression

602 summaries in (I) CD45, (J) CD4, and (K) CD8 cells. Data (A-E) combined from three

603 independent experiments (n=15). Data (F-K) are representative of two independent experiments

604 (n=5). Data (A-K) were analyzed by ordinary one-way ANOVA with Tukey's multiple

605 comparisons test and represented as mean ± SEM. Non-significant [ns], *$p < 0.05$, **$p < 0.01$,

606 ***$p < 0.001$, ****$p < 0.0001$.

607

608

609

610

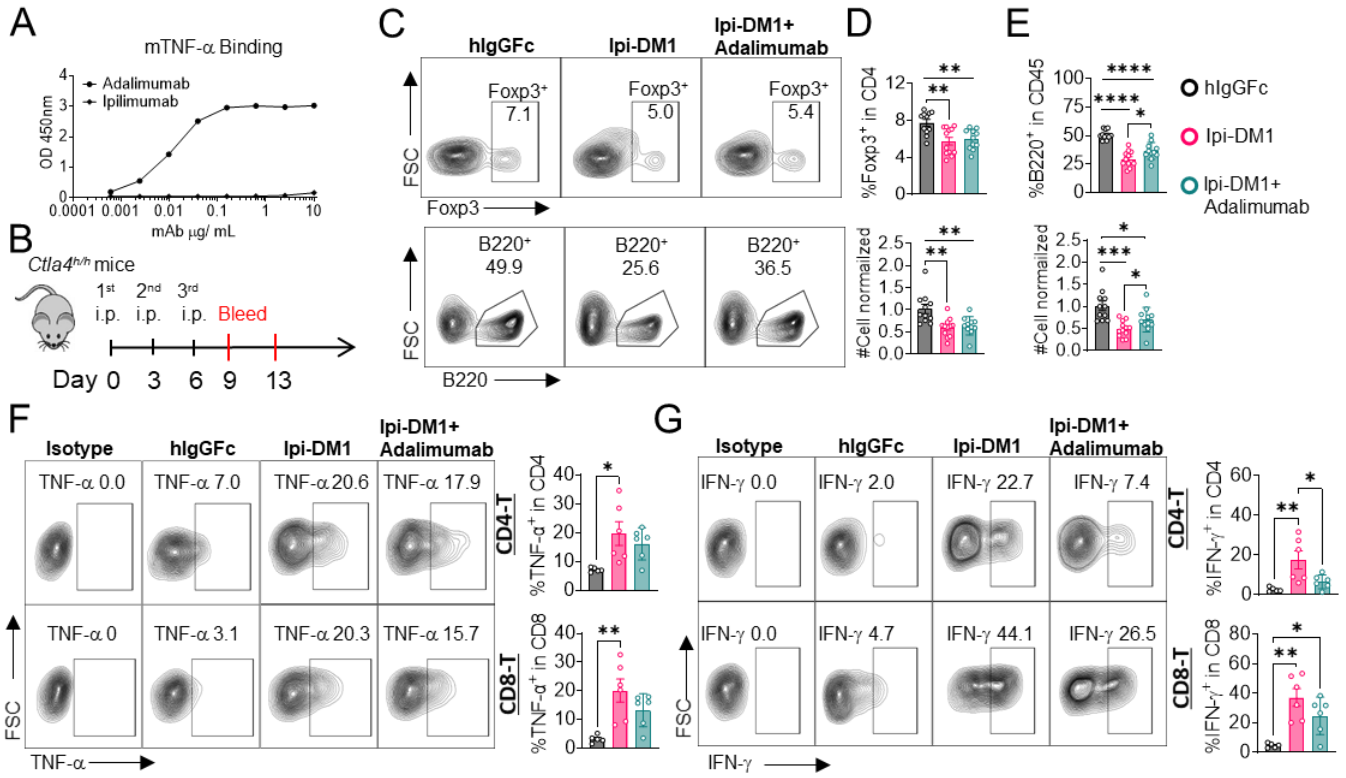

Figure 6. B-cell depletion is partially rescued by anti-TNF-alpha.

(A) ELISA binding of clinical grade drug Adalimumab (Humira) to pre-coated 1µg/mL mouse-TNF-alpha and detected with anti-hIgG-HRP, Ipilimumab negative control. (B) Diagram of experimental design, male *Ctla4*$^{h/h}$ mice were treated intraperitoneal (i.p.) (100 µg/mouse) with hIgGFc or Ipi-DM1 with/out (100 µg/mouse of Adalimumab) every three days for total of three doses and mice were bled on day 9 and 13. (C) FACS profiles depicting gating strategy after gating on CD45 for Tregs (% Foxp3^{+} in CD4) (top panel) and B cells (% B220^{+} in CD45) (bottom panel) from day 9 peripheral blood. (D) % Foxp3^{+} (Tregs) in CD4 and normalized cell number. (E) % B220^{+} in CD45 and normalized cell number. (F, G) Day 13 peripheral blood post red blood lysis by ACK buffer were cultured and stimulated in the presence of Ononmycin/PMA, and GolgiPlug for 4 hrs followed by intracellular cytokine detection (TNF-alpha, IFN-gamma) in CD4 and CD8 T cells, (F) TNF-alpha, and (G) IFN-gamma. Data (C-E)

are combined from two independent experiments (n=11-12) and analyzed using an unpaired two-tailed Student's t test and represented as mean ± SEM. *$p < 0.05$, **$p < 0.01$, ***$p < 0.001$, ****$p < 0.0001$. Data (F, G) is representative of two independent experiments (n=5-6) and analyzed by ordinary one-way ANOVA with Tukey's multiple comparisons test and represented as mean ± SEM. *$p < 0.05$, **$p < 0.01$, ***$p < 0.001$, ****$p < 0.0001$.

Table 1 Drug to antibody ratio (DAR)

Entry	A_{280}	A_{252}	CmAb (Moles)	CDM1(Moles)	DAR CDM1/CmAB
hIgGFC-DM1	0.51	0.48	6.92705E-06	1.1531E-05	1.7
Ipilimumab-DM1	0.62	0.42	2.30582E-06	7.32032E-06	3.2

Drug to antibody ratio (DAR)= CDM1/ CmAB. DM1 known extinction coefficients (A_{280}, 5700 $M^{-1}cm^{-1}$; A_{252}, 28084 $M^{-1}cm^{-1}$). Experimentally derived extinction coefficients for Ipilimumab (A_{280}, 242115 $M^{-1}cm^{-1}$; A_{252}, 92989 $M^{-1}cm^{-1}$) and hIgGFc (A_{280}, 64136 $M^{-1}cm^{-1}$; A_{252}, 22544 $M^{-1}cm^{-1}$)

638

639 **Table S1. Drug to antibody ratio (DAR)**

640

641

642

643

644

645

646

647

648

649

650

651

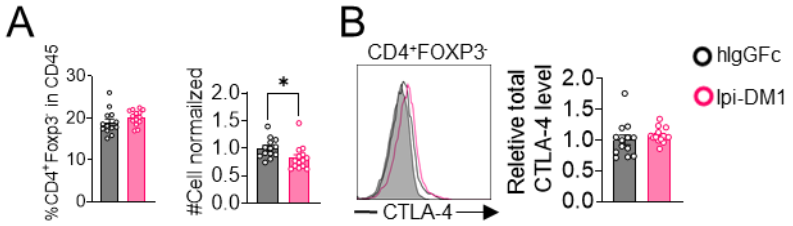

Figure 1-figure supplement 1. CD4-nonTregs and CTLA-4 expression.

(A) % $CD4^{+}$ $Foxp3^{-}$ in CD45 and normalized cell number. (B) Relative CTLA-4 level in CD4-nonTregs. Data combined from two independent experiments (n=13-14) and analyzed using an unpaired two-tailed Student's t test and represented as mean ± SEM. *$p < 0.05$, **$p < 0.01$, ***$p < 0.001$, ****$p < 0.0001$.

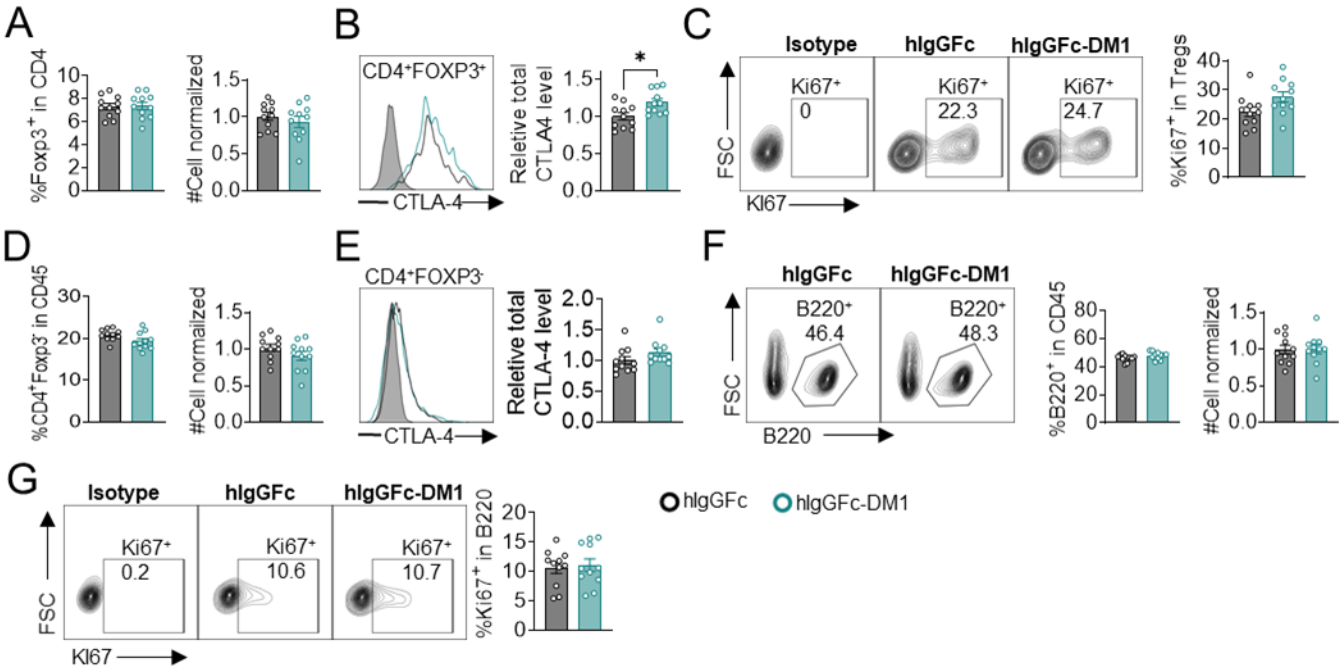

Figure 1-figure supplement 2. B-cell depletion is not mediated by DM1 payload off-target release.

(A) % Foxp3^{+} in CD4 and normalized cell number. (B) Relative CTLA-4 level in Tregs. (C) % Ki67^{+} in Tregs. (D) % CD4^{+} Foxp3^{-} in CD45 and normalized cell number. (E) Relative CTLA-4 level in CD4-nonTregs. (F) FACS profiles depicting gating strategy after gating on CD45^{+} and data summaries of % B220^{+} in CD45 and normalized cell number. (G) % Ki67^{+} in B cells. Data combined from two independent (n=11) and analyzed using an unpaired two-tailed Student's t test and represented as mean ± SEM. *$p < 0.05$, **$p < 0.01$, ***$p < 0.001$, ****$p < 0.0001$.

670

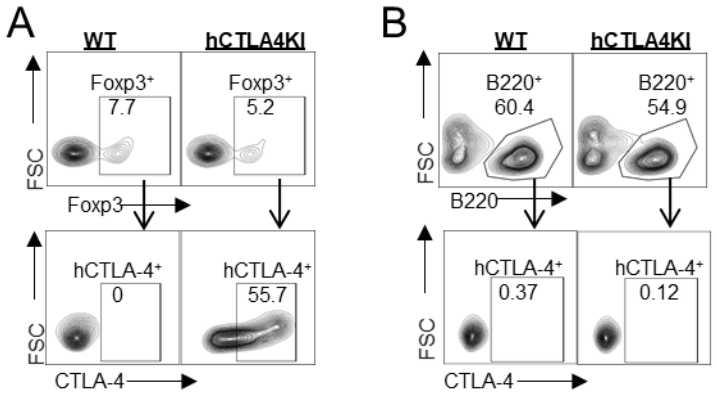

671 **Figure 1-figure supplement 3. B-cells do not express CTLA-4.**

672 FACS profile of human CTLA-4 in wild-type and human CTLA-4 knock-in mice peripheral

673 blood, (A) % CTLA-4^{+} in Tregs (CD45^{+} CD4^{+} Foxp3^{+}), and (B) % CTLA-4^{+} in B cells (CD45^{+}

674 B220^{+}). Data representative of 2 mice.

675

676

677

678

679

680

681

682

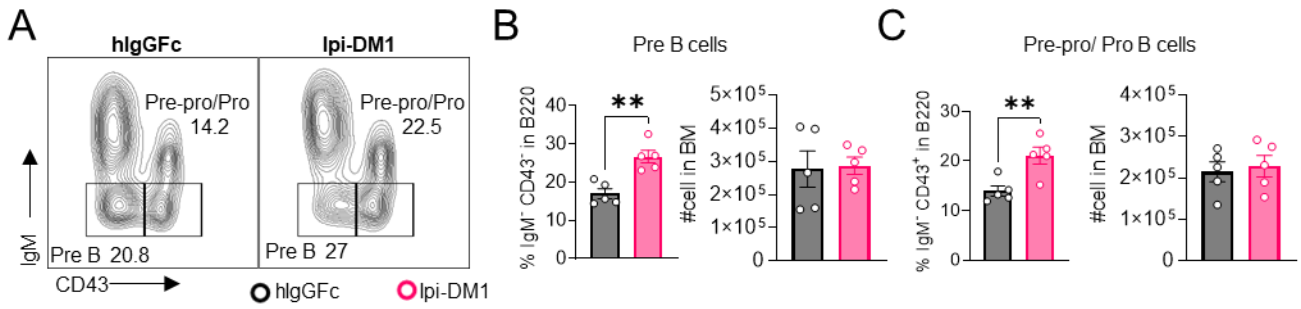

Figure 1-figure supplement 4. IgM negative B-cell subtypes in bone marrow.

(A) FACS profile gating of Pre B (IgM^-CD43^-) and Pre-pro/Pro (IgM^-CD43^+) cells in B220. (B-C) % of B cell subtype in B220 and absolute cell numbers, (B) Pre B cells, (C) Pre-pro/Pro B cells. Data is representative of one experiment (n=5) and analyzed using an unpaired two-tailed Student's t test and represented as mean ± SEM. *$p < 0.05$, **$p < 0.01$, ***$p < 0.001$, ****$p < 0.0001$.

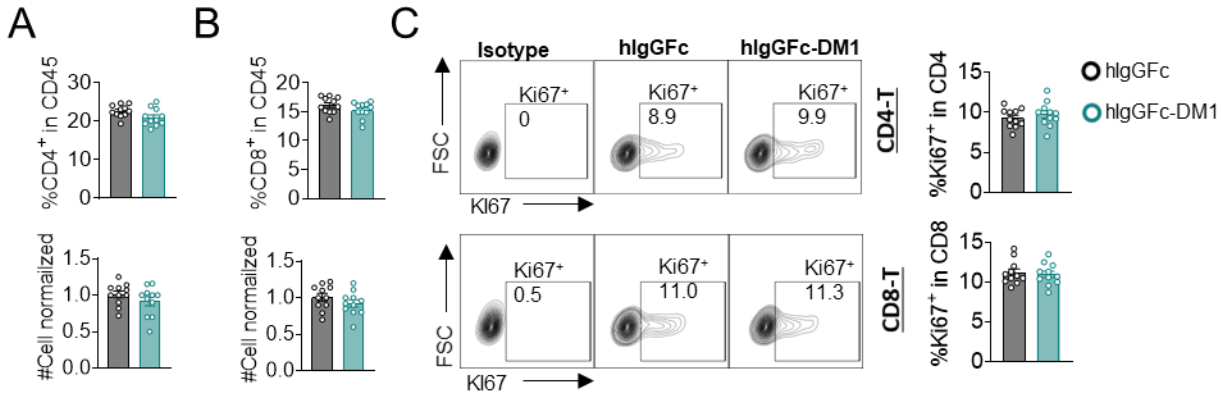

Figure 3-figure supplement 1. T-cell quantity and proliferation are not impacted by IgG-DM1 treatment.

(A) % $CD4^+$ in CD45 and normalized cell number. (B) % $CD8^+$ in CD45 and normalized cell number. (C) % $Ki67^+$ in CD4 and CD8 T cells. Mice treated with hIgGFc or hIgGFc-DM1, data combined from two independent experiments (n=11) and analyzed using an unpaired two-tailed Student's t test and represented as mean ± SEM. *$p < 0.05$, **$p < 0.01$, ***$p < 0.001$, ****$p < 0.0001$.

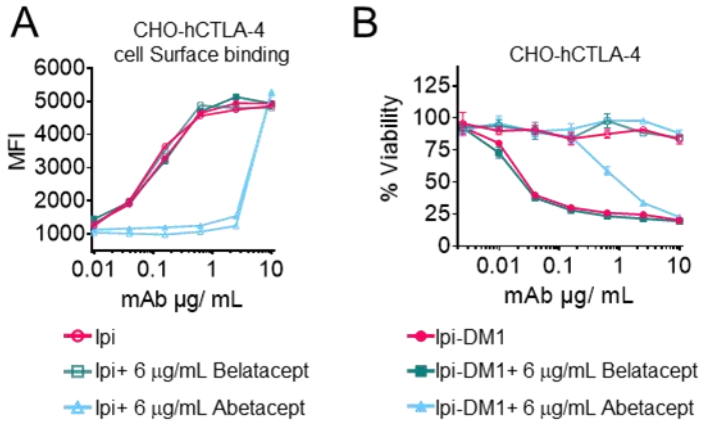

Figure 5-figure supplement 1. Mutant soluble CTLA-4-Ig does not neutralize Ipilimumab or its drug-conjugate.

(A) Detached CHO cells expressing hCTLA-4 were incubated with serial dilution of Ipi or Ipi-DM1 in the presence of given dose of Abatacept or Belatacept on ice for 30 minutes followed by FACS detection using mouse anti-human IgG AF488, mean fluorescence intensity (MFI) . (B) MTT cell viability of CHO-hCTLA-4 cells after 72 hours incubation with Ipi or Ipi-DM1 in the presence of given dose of Abatacept or Belatacept. Data is representative of two independent experiments (n=3).

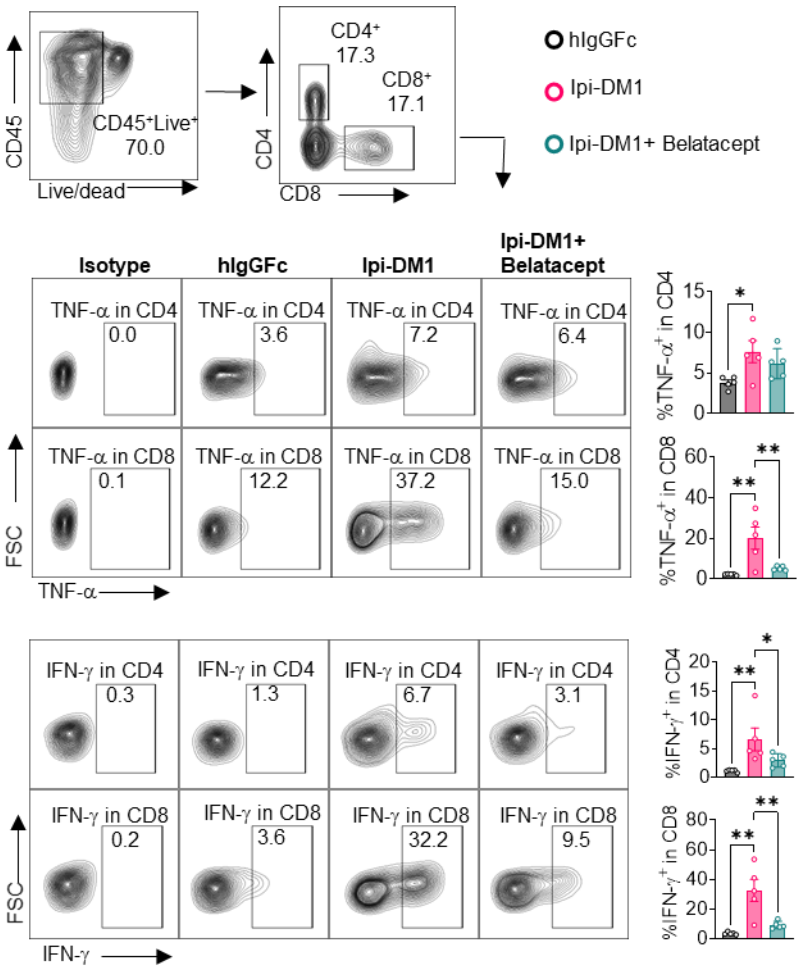

Figure 5-figure supplement 2. T-cell cytokine production.

Day 13 peripheral blood samples from treated (hIgGFc or Ipi-DM1 with/out Belatacept) mice post ACK buffer red blood lysis were cultured and stimulated in the presence of Ononmycin/PMA, and GolgiPlug for 4 hrs followed by intracellular cytokine detection (TNF-alpha, IFN-gamma) in CD4 and CD8 T cells. Data is representative of two independent experiments (n=5) analyzed by ordinary one-way ANOVA with Tukey's multiple comparisons test and represented as mean ± SEM. *$p < 0.05$, **$p < 0.01$, ***$p < 0.001$, ****$p < 0.0001$.

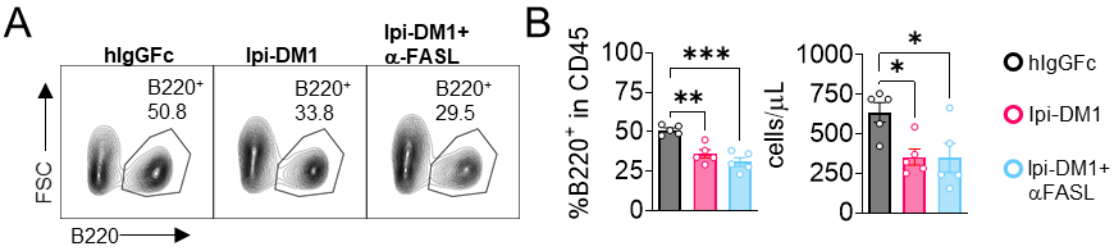

Figure 6-figure supplement 1. Anti-FASL fails to rescue B cell.

Ctla4$^{h/h}$ mice were treated intraperitoneally (i.p.) (100 µg/mouse) with hIgGFc or Ipi-DM1 with/out (100 µg/mouse of anti-FASL) every three days for a total of three doses and mice were bled on day 9. (A) FACS profile after gating on CD45 for B cells. (B) % B220^{+} in CD45 and absolute B cell number summaries. Data is representative of one experiment (n=5). Data analyzed by ordinary one-way ANOVA with Tukey's multiple comparisons test and represented as mean ± SEM. *$p < 0.05$, **$p < 0.01$, ***$p < 0.001$, ****$p < 0.0001$.